

A mouse *Mecp2*-null mutation causes neurological symptoms that mimic Rett syndrome

Jacky Guy¹, Brian Hendrich¹, Megan Holmes², Joanne E. Martin³ & Adrian Bird¹

Rett syndrome (RTT) is an inherited neurodevelopmental disorder of females that occurs once in 10,000–15,000 births^{1,2}. Affected females develop normally for 6–18 months, but then lose voluntary movements, including speech and hand skills. Most RTT patients are heterozygous for mutations in the X-linked gene *MECP2* (refs. 3–12), encoding a protein that binds to methylated sites in genomic DNA and facilitates gene silencing^{13–17}. Previous work with *Mecp2*-null embryonic stem cells indicated that MeCP2 is essential for mouse embryogenesis¹⁸. Here we generate mice lacking *Mecp2* using Cre-*loxP* technol-

ogy. Both *Mecp2*-null mice and mice in which *Mecp2* was deleted in brain showed severe neurological symptoms at approximately six weeks of age. Compensation for absence of MeCP2 in other tissues by MeCP1 (refs. 19,20) was not apparent in genetic or biochemical tests. After several months, heterozygous female mice also showed behavioral symptoms. The overlapping delay before symptom onset in humans and mice, despite their profoundly different rates of development, raises the possibility that stability of brain function, not brain development *per se*, is compromised by the absence of MeCP2.

Previous attempts to create *Mecp2*-null mice using *Mecp2*^{-/-} ES cells were unsuccessful¹⁸. To circumvent the problem of embryonic lethality, we replaced exons 3 and 4 of *Mecp2* in ES cells with the same exons flanked by *loxP* sites²¹ (Fig. 1a). Mice homozygous or hemizygous for the replacement were viable and fertile. Northern blots showed the expected mature transcript from the *Mecp2*^{lox} locus (2.5 kb) plus a transcript in which the β -globin intron was unspliced (3.3 kb; Fig. 1b). Early embryonic deletion of the gene was achieved by crossing *Mecp2*^{lox/lox} females with deleter mice, which express Cre ubiquitously²². Southern blots showed that recombination between *loxP* sites had occurred in all female offspring carrying the deleter transgene and the *Mecp2*^{lox} allele (Fig. 1d), leading to deletion of all but the amino-terminal eight amino acids of MeCP2. When *Mecp2*^{+/-} females were mated with wild-type C57BL/6 males, equal numbers of wild-type and

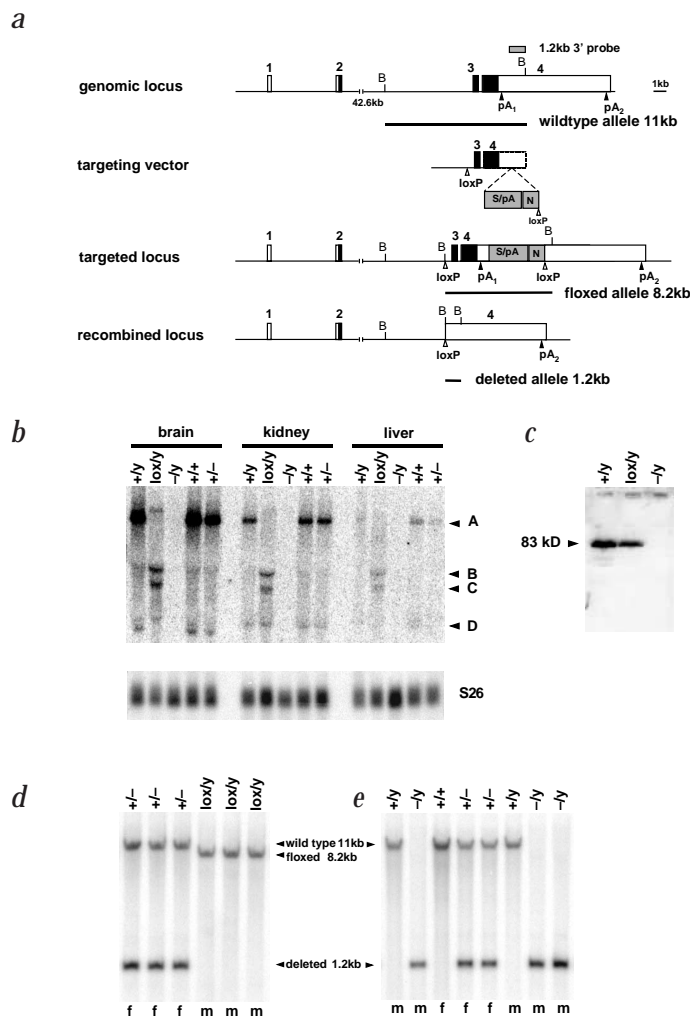


Fig. 1 Disruption of mouse *Mecp2* using Cre-*loxP* technology. **a**, Maps of the genomic locus, targeting vector, targeted locus and recombined locus after exposure to Cre. **b**, Northern blot analysis of RNA from brain, kidney and liver of wild-type male (+/y), floxed male (lox/y), *Mecp2*-null male (-/y), wild-type female (+/+) and female heterozygous for the null allele (+/-) probed with a 3.2-kb *NcoI* fragment including exons 3 and 4 of *Mecp2*. Bands A (10 kb) and D (2 kb) are seen in wild-type tissue, whereas bands B (3.3 kb) and C (2.5 kb) are due to transcription of the floxed *Mecp2* allele. No *Mecp2* mRNA is detected in the null males. Equal loading of RNA is demonstrated by hybridization of the same blot to an S26 ribosomal protein mRNA probe. **c**, Western blots of brain protein from wild-type, floxed and null mice. No MeCP2 protein is detected in *Mecp2*-null brain. **d**, Southern blots of DNA from tails of a single litter derived from a cross between a *Mecp2*^{lox/lox} female and a male carrying the X-linked deleter transgene. Females, but not males, have deleted the floxed allele in tail cells as expected. **e**, Southern blot analysis of tail DNA from mice born to a cross between a *Mecp2*^{+/-} female and a wild-type male. Half of males are expected to be *Mecp2*^{-y}.

¹Wellcome Centre for Cell Biology, Institute of Cell and Molecular Biology, University of Edinburgh, The King's Buildings, Edinburgh, UK. ²Department of Clinical Neurosciences, Molecular Medicine Centre, University of Edinburgh, Western General Hospital, Edinburgh, UK. ³St Bartholomews and the Royal London School of Medicine and Dentistry, Queen Mary and Westfield College, The Institute of Pathology, The Royal London Hospital, Whitechapel, London, UK. Correspondence should be addressed to A.B. (e-mail: a.bird@ed.ac.uk).

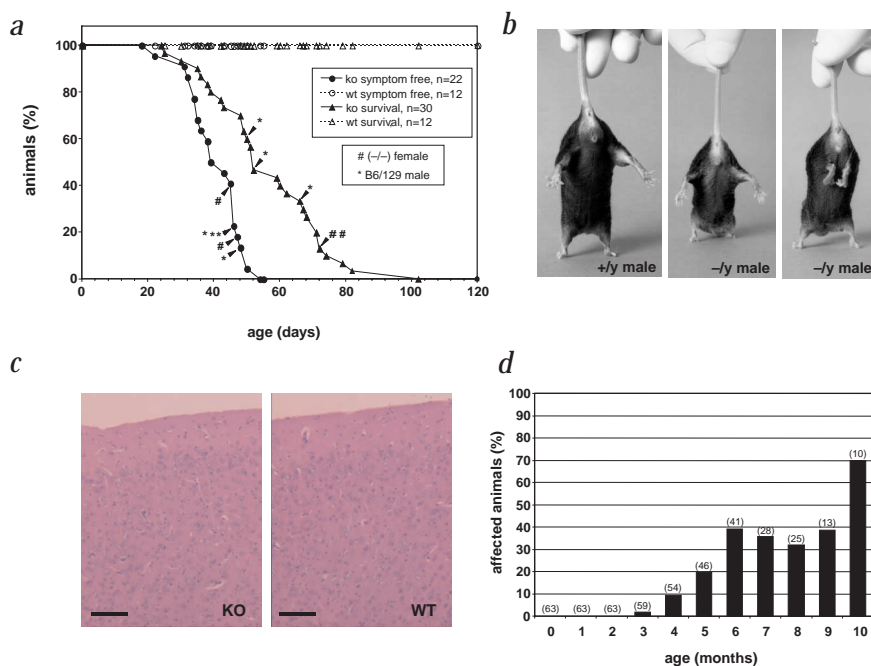


Fig. 2 Phenotypes of mice with the *Mecp2*-null mutation. **a**, Cumulative plot showing percentage of wild-type (open symbols) and hemizygous or homozygous *Mecp2*-null animals (filled symbols) that survived (triangles) or remained free of obvious neurological symptoms (circles) with increasing time. Most data concerns *Mecp2*^{-y} males on a C57BL/6 background, but the timings for *Mecp2*^{-y} males crossed with 129 mice (*) and for *Mecp2*^{-/-} females (#) are highlighted. **b**, Delayed onset hind limb claspings in *Mecp2*^{-y} males. The left and middle panels show normal spreading of hindlimbs in wild-type and six-week mutant males, respectively. Right, limb-clasping phenotype in a mutant male aged 7 weeks. **c**, Sections showing histology of cerebral cortex of a 10-week *Mecp2*^{-y} mouse with pronounced neurological symptoms (KO) and an age-matched wild-type control (WT) stained with hematoxylin and eosin. Scale bar, 50 μ m. **d**, Histogram showing fraction of female mice heterozygous for the *Mecp2*-null mutation that exhibit neurological symptoms in different age groups (number in group shown in brackets).

Mecp2^{-y} males were born (Fig. 1e). No *Mecp2* mRNA or protein was detected in tissues from *Mecp2*^{-y} mice (Fig. 1b,c). We obtained *Mecp2*^{-/-} females by crossing *Mecp2*^{+/-}, deleter^{+/-} females with *Mecp2*^{lox/y} males (data not shown). The viability of *Mecp2*-null animals proves that absence of MeCP2 does not cause embryonic lethality in mice, contrary to a previous conclusion¹⁸. The inviability of chimeric embryos containing *Mecp2*-null ES cells seen previously may be due to adverse effects of the inserted *lacZ* transgene on linked genes, or to epigenetic changes that reduce pluripotency arising during ES proliferation in the absence of MeCP2.

Mecp2-null male and female mice showed no initial phenotype, but both developed a stiff, uncoordinated gait and reduced spontaneous movement between three and eight weeks of age (Fig. 2a). Most animals subsequently developed hindlimb claspings (Fig. 2b) and irregular breathing. Uneven wearing of the teeth and misalignment of the jaws was also frequent. Testes of *Mecp2*-null males were always internal. Neither motor defects nor sensory defects were detected, but some affected animals failed to respond to sound. Pathological analysis of symptomatic animals revealed no obvious histological abnormalities in a range of organs. In particular, the brain showed no unusual features of cortical lamination, ectopias or other abnormalities (Fig. 2c). Variable progression of symptoms lead ultimately to rapid weight loss and death at approximately 54 days (Fig. 2a).

A distinct feature of the phenotype was varying body weight, which was dependent on genetic background. The *Mecp2*-null mutation on a C57BL/6 background gave rise to animals that were substantially underweight from four weeks with full penetrance (Fig. 3a-c). After crossing to a 129 strain, however, F1 animals showed a reverse effect. Instead of losing weight, *Mecp2*^{-y} mice were the same weight as wild-type littermates until eight weeks, when survivors became significantly heavier than siblings (Fig. 3d) with an obvious increase in deposited fat. Other aspects of the phenotype, including behavioral defects, were not affected by altered genetic background. These data indicate the presence of one or more modifier genes that mediate the effects of MeCP2 on body weight.

Mecp2 is expressed in many mouse tissues, but the phenotype of *Mecp2*-null mice suggests neurological defects. To test whether the effects of MeCP2 loss are specific to brain, the mutation was combined with the nestin-Cre transgene²³, which is highly expressed in neuronal and glial cells. Southern blots confirmed that *Mecp2*^{lox} was approximately 65% deleted in brain (85% in cerebellum), but 10% deleted or less in other somatic tissues (Fig. 3e). The phenotype of mice with extensive deletion of *Mecp2* in brain was indistinguishable from that of *Mecp2*-null mice. The low frequency of *Mecp2* deletion in non-brain tissues is unlikely to contribute to the phenotype, as *Mecp2*^{+/-} females are mosaic for *Mecp2* expression due to X-chromosome inactivation, yet show no phenotype at this age. These data indicate that the major features of the *Mecp2*-null phenotype, including reduced movement, abnormal gait, limb claspings, low weight (Fig. 3f), internal testes, uneven wearing of teeth and lethality, are probably due to absence of MeCP2 in neuronal and/or glial cells.

The brain-specific effects of *Mecp2* deletion may be due to compensation for lack of MeCP2 in other tissues by a different methyl-CpG binding repressor. *Mbd2* is a component of the MeCP1 histone deacetylase complex, which also represses transcription²⁰. As *Mbd2*^{-/-} mice are viable and fertile²⁴, we tested for a possible interaction between MeCP2 and *Mbd2* by combining the *Mecp2*-null and *Mbd2*-null mutations. Double-mutant animals showed the same onset of symptoms and mortality as single-mutant *Mecp2*-null mice, providing no evidence for a genetic interaction between *Mecp2* and *Mbd2* (Fig. 4a).

We further analysed repression of methylated reporter genes in tail fibroblast cell lines from wild-type mice and mice lacking *Mecp2*, *Mbd2*, or both. Repression was only marginally reduced in *Mecp2*^{-y} cells (~5% of the non-methylated control) compared with wild-type cells (~2%; Fig. 4b). *Mbd2*^{-/-} cells, in contrast, repressed methylated reporter genes inefficiently (25–30% of non-methylated control²⁴), but this incomplete repression was unaltered in double-mutant *Mbd2*^{-/-}, *Mecp2*^{-y} cells. By these assays, therefore, methyl-CpG-dependent repression in tail fibroblasts is due to *Mbd2*, and MeCP2 has a minimal role. Expression of exogenous MeCP2 did, however, restore full repression to *Mbd2*^{-/-} cells, demonstrating that

letter

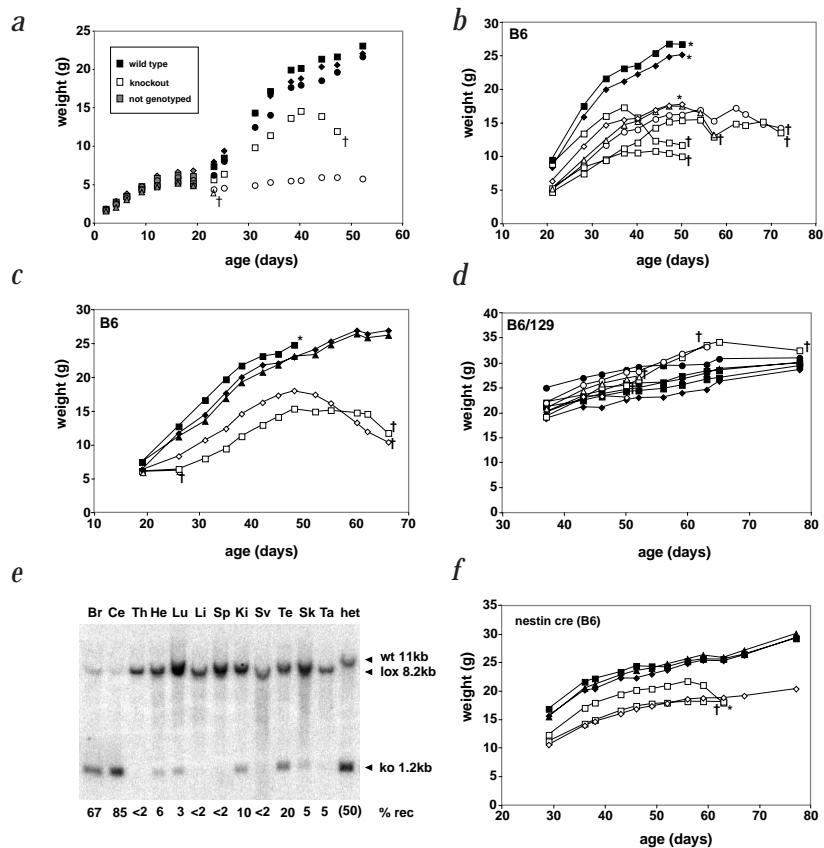


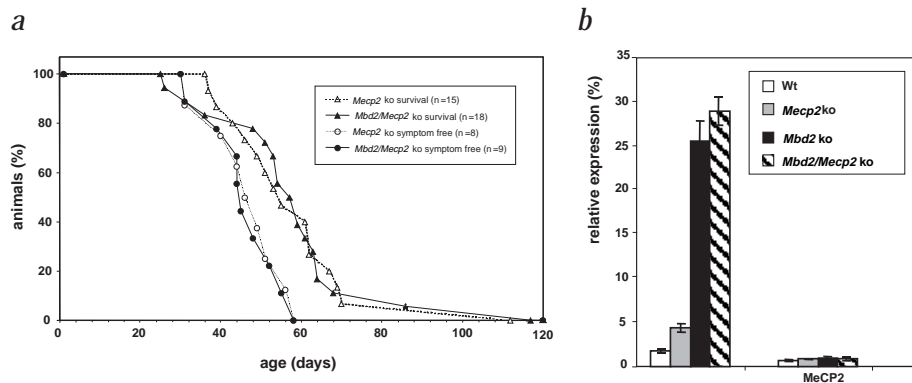
Fig. 3 Effects of *Mecp2* deletion on body weight. **a**, Body weight from birth of individual males from a single litter. *Mecp2*-null males are significantly smaller than wild-type littermates from around weaning (~3 weeks of age). **b, c**, Body weight from weaning of two different litters on a C57BL/6 (B6) background, showing reduced weight of *Mecp2*-null animals (open symbols) compared with wild-type littermates (filled symbols). **d**, Body weight of *Mecp2*^{-/-} (open symbols) and wild-type (filled symbols) littermates on a C57BL/6×129 F1 background. The two mutant animals (of 4 in the litter) surviving beyond 7 weeks gained weight relative to littermates. **e**, Southern blot analysis of tissue DNA from a male mouse containing the nestin-Cre transgene and the floxed allele of *Mecp2*. The proportion of recombination in each tissue is calibrated by comparison with band intensities in DNA from a heterozygote for the wild-type and null alleles (het), where the ratio is known to be 1:1. The tissues tested are brain (minus cerebellum) (Br), cerebellum (Ce), thymus (Th), heart (He), lung (Lu), liver (Li), spleen (Sp), kidney (Ki), seminal vesicles (Sv), testis (Te), skeletal muscle (Sk) and tail (Ta). Percentage of chromosomes deleted is shown below each lane. **f**, Body weight from weaning of C57BL/6 *Mecp2*^{lox/y} males (open symbols) carrying a nestin-Cre transgene that causes deletion of *Mecp2* predominantly in brain (**e**) compared with wild-type littermates (filled symbols). Reduced weight like that seen for *Mecp2*^{-/-} males is apparent, indicating a neurological origin for this component of the phenotype. **d–f**, Animals dying naturally (†) and those sacrificed for experimental reasons (*) are indicated.

MeCP2 can act as a methyl-CpG-dependent repressor in this system (Fig. 4b). The combined genetic and biochemical results indicate that Mbd2 and MeCP2 function in independent pathways. It remains possible that another methyl-CpG binding repressor (for example, Mbd1; refs. 25,26) might compensate for absence of MeCP2.

Although *Mecp2*^{+/-} female mice initially showed no symptoms and raised normal litters, they acquired the inertia and hindlimb clasp phenotypes at ages greater than three months (Fig. 2d). By nine months of age, about one-half of the heterozygous mice showed unambiguous symptoms, often including breathing irregularities, but some remained asymptomatic at one year. The

overlapping delay seen in mice and humans before onset of the effects of *Mecp2* mutation is unexpected given the different timing of their developmental programmes. The mobility of affected animals was quantified using an open field test²⁷. Symptomatic heterozygotes visited fewer squares, spent more time being immobile and reared less than age-matched wild-type controls (Table 1). This was not due to heightened anxiety, as fecal bolus counts, grooming times and time spent in different zones of the field were similar to those of controls. Unlike *Mecp2*-null animals, heterozygotes did not undergo rapid deterioration, raising the possibility that the *Mecp2*^{+/-} condition can, like RTT, exhibit long-term stability.

Fig. 4 Absence of obvious genetic or biochemical interactions between MeCP2 and the methyl-CpG binding repressor Mbd2. **a**, Cumulative plot comparing percentage of *Mecp2*^{-/-} (open symbols) and *Mecp2*^{-/-}, *Mbd2*^{-/-} double-mutant animals (filled symbols) that survived (triangles) or remained free of neurological symptoms (circles) with increasing time. The profiles for the two genotypes were determined in parallel using littermates on a C57BL/6×129 background (B6/129) and are independent of the data shown in Fig. 2a. **b**, Repression of a methylated reporter construct containing the pGL2 promoter relative to the same reporter unmethylated, is only slightly less efficient in *Mecp2*^{-/-} cells than in wild-type cells. Relative repression is significantly less efficient in *Mbd2*^{-/-} cells and this efficiency is not reduced in double-mutant *Mecp2*^{-/-}, *Mbd2*^{-/-} cells. Co-transfection with an MeCP2 expression construct (right) restores repression of the methylated reporter gene.





The results of this and the accompanying paper²⁸ show that mice with the *Mecp2*-null mutation are a valid model for human RTT, as delayed onset of a neurological crisis affecting gait, posture, breathing and spontaneous movement is seen in both conditions. These data support the view that RTT is primarily a neurological disease, but in other respects they challenge current perceptions of this condition. First, it has been thought that RTT is caused by mutations that impair the function of MeCP2, but do not inactivate it. Advanced mouse development in the absence of MeCP2, plus evidence that certain human *MECP2* mutations apparently abolish the function of the protein^{29,30}, argue that many RTT patients may be heterozygous for what are effectively null mutations in *MECP2*. A second unexpected finding is that the absolute time of onset of symptoms overlaps in human and mouse *MECP2* heterozygotes. This approximate correspondence in real time, not developmental time, argues against a developmental defect due to MeCP2 deficiency, as this would arise much earlier in rapidly developing mice. An alternative hypothesis is that neurogenesis can be accomplished in the absence of MeCP2, but that the resulting brain cells, whether human or mouse, are functionally unstable. Brain function in *MECP2*-null males of either species may therefore decline steeply, leading to early symptoms and death. Heterozygous females, on the other hand, have many brain cells that express wild-type MeCP2 and would therefore take longer to reach the level of brain cell dysfunction at which neurological symptoms appear.

Methods

Conditional gene targeting construct. The targeting vector was designed to flank the coding sequences in exons 3 and 4 (all but the first 8 aa of the protein) with *loxP* sites, also adding an additional intron and polyadenylation signal from the human β -globin gene and a neomycin resistance gene for selection of transfected ES cells. The targeting vector was constructed using a 7.2-kb *Bam*HI genomic fragment subcloned in pBSIKS+ from a 40-kb 129 mouse cosmid. The 3' *Bam*HI site is present in the mouse genome, with the 5' site coming from the cosmid polylinker. The 5' *loxP* site and diagnostic restriction sites were inserted into a *Nco*I site in intron 2 using oligonucleotides. A second *Nco*I site in the 3' UTR was used to insert a 2.8-kb *Bam*HI-*Xba*I fragment containing intron 2 and the polyadenylation signal of human β -globin, followed by a 1.2 kb TK-neo cassette flanked by *loxP* sites ("floxed"; a gift from A. Smith). This resulted in a targeting vector with ~2.8 kb of 5' homology, 1.2 kb of 3' homology and a 3.2-kb floxed segment. The vector was linearized for transfection at the 3' end using *Xho*I.

ES cell culture and gene targeting. We carried out gene targeting in the ES cell line E14 TG2a (A. Smith) which is derived from the mouse substrain 129/Ola. Cells were grown on gelatinized dishes without feeder cells in the presence of recombinant human LIF (a gift from A. Smith) in Glasgow MEM (Life Technologies) supplemented with 10% fetal bovine serum (GlobePharm), 1×MEM non-essential amino acids, sodium pyruvate (1 mM), β -mercaptoethanol (50 μ M; all Life Technologies). ES cells (5×10⁷ cells) were transfected with the linearized targeting vector (250 μ g DNA in 0.8 ml HEPES buffered saline) by electroporation (800 V, 3 μ F, BioRad Gene Pulser) and plated in 10-cm dishes at 5×10⁶ cells per dish. Correctly targeted clones were identified by Southern-blot analysis. For targeting at the 3' end, ES-cell DNA was digested with *Bam*HI and the blots probed with a 1.2-kb *Nco*I-*Bam*HI fragment. The 11-kb wild-type band was replaced in targeted clones by a 8.2-kb band from the floxed allele. To check

Table 1 • Performance of wild-type and *Mecp2*^{+/-} females in open field testing

	Wild type ^a	Heterozygote ^a	<i>P</i> = ^b
Number of animals	7	11	–
Total no. squares visited	139 (16)	73 (14)	0.0087
% Squares visited ^c			
outer	80.8 (2.7)	80.4 (4.3)	NS
middle	14.6 (2.3)	15.4 (4.1)	NS
inner	4.5 (0.8)	4.3 (1.4)	NS
Number of rears	15.9 (4.4)	4.3 (1.3)	0.0078
Number of fecal boli	2.7 (0.8)	3.6 (0.5)	NS
Time spent grooming (s)	14.5 (2.8)	9.2 (1.9)	NS
Time spent immobile (s)	27.9 (5.2)	90.3 (18.2)	0.0172

^aMean values are shown followed by the standard error of the mean in brackets. ^bValues for wild-type and heterozygous females were compared using an unpaired *t*-test. Where a significant difference was found at the 95% confidence level, the *P* value is shown. NS indicates 'not significant'. ^cThe squares of the open field apparatus were classified as outer, middle or inner.

for the presence of the 5' *loxP* site, the same *Bam*HI-digested DNA was probed with a 0.95-kb *Xba*I-*Nco*I fragment. The wild-type allele gave an 11-kb band, the targeted gene without 5' *loxP* site, a 15-kb band, and the targeted gene with 5' *loxP* site, a 6.8-kb band.

Generation and breeding of chimeric mice. Correctly targeted ES cell clones for injection into blastocysts were passaged the day before injection and injected into blastocysts from naturally mated C57BL/6 females at 3.5 days post coitum. Injections were performed in M2 medium (Sigma) with 10–15 ES cells being injected into each blastocyst before transfer to pseudopregnant recipient females (6–12 blastocysts per recipient). Chimeric pups were identified by their agouti coat color and, on maturity, were mated with C57BL/6 mice. As *Mecp2* is X-linked, all agouti F1 females were heterozygous for the floxed allele, and this was confirmed by Southern blot. We crossed heterozygous females with wild-type C57BL/6 males (F2 generation). Resulting hemizygous males were crossed to heterozygous females to generate homozygous females (F3) and the line was then maintained in the homo/hemizygous state.

Cre-expressing mice and deletion of *Mecp2*. We obtained deleter mice²², which carry a ubiquitously expressed Cre transgene on the X chromosome. Male deleter mice were crossed with homozygous floxed females. All female pups were *Mecp2*^{+/-} and hemizygous for *cre*. All male pups were hemizygous for the *Mecp2*^{lox} allele. *Mecp2*^{+/-} females were crossed with wild-type C57BL/6 males to give *Mecp2*^{+/-} or *Mecp2*^{+/+} females and *Mecp2*^{+/-} or *Mecp2*^{-/-} males. The three *Mecp2* alleles were identified by Southern-blot analysis by digesting with *Bam*HI and probing with the 1.2-kb *Nco*I-*Bam*HI 3' probe (*Mecp2*⁺, 11 kb; *Mecp2*^{lox}, 8.2 kb; *Mecp2*⁻, 1.2 kb). Heterozygous nestin-Cre males²³ were crossed with *Mecp2*^{lox/lox} females to generate males that had *Mecp2* deleted in neural and glial cells. Animals carrying the nestin-Cre transgene were identified by PCR on tail genomic DNA (forward primer CreF, 5'–GACCGTACACCAAATTTGGCTG–3'; reverse primer CreR, 5'–TTACGTATATCCTGGCAGCGATC–3'; 5 min at 94 °C, 30 cycles of 30 s at 94 °C, 30 s at 64 °C, 45 s at 72 °C, followed by 5 min at 72 °C. The 465-bp product was visualized by running on a 1.5% TAE agarose gel. Various tissues were used to make genomic DNA, which was digested with *Bam*HI, Southern blotted and probed with the *Nco*I-*Bam*HI 3' *Mecp2* probe. The extent of deletion in each tissue was quantified using ImageQuant software (Molecular Dynamics), correcting for background and higher intensity signal from the smaller, deleted allele.

Southern-, northern- and western-blot analysis. Genomic DNA was prepared from ES cell clones and tail tips by standard procedures. RNA was prepared from mouse tissues using TriReagent (Sigma) following homogenization in an UltraTurrax homogenizer. RNA was made from the lysates according to the manufacturer's protocol. Southern and northern blots were prepared by standard procedures. Radioactive probe was detected using a PhosphorImager (Molecular Dynamics) and quantitated using ImageQuant software.

We carried out western-blot analysis on total brain extracts from wild-type, floxed and mutant mice. Brains were collected in cold PBS and transferred to cold Laemmli sample buffer without SDS (60 mM Tris Cl, pH 6.8, 100 mM DTT, 10% glycerol). The tissue was then homogenized using an UltraTurrax on high speed for 10 s before adding SDS to 2%. Lysates were sonicated briefly, boiled for 5 min and centrifuged for 10 min at 13,000 r.p.m. Super-



letter

natant aliquots were run on 12.5% SDS-PAGE gels with 10 µg protein per lane. Western blots with anti-MeCP2 rabbit polyclonal antibody (Upstate Biotech) were carried out according to the manufacturer's instructions and visualized on Hyperfilm using the ECL system (Amersham).

Transient transfection assays. We used tail fibroblasts with the following four genotypes: *Mecp2^{+/y}, Mbd2^{+/+}*; *Mecp2^{-/y}, Mbd2^{+/+}*; *Mecp2^{+/y}, Mbd2^{-/-}*; and *Mecp2^{-/y}, Mbd2^{-/-}*. *Mbd2^{-/-}* cells were obtained as described²⁴. *Mecp2^{-/y}* cells were obtained by immortalizing tail fibroblasts from *Mecp2^{lox/y}* males on either an *Mbd2^{+/+}* or *Mbd2^{-/-}* background and subsequently transfecting with a CMVcre transgene. Cell clones that had deleted *Mecp2* were then selected. Cells were grown to approximately 50% confluence and transfected using Lipofectamine according to the manufacturer's instructions (Life Technologies). Each well of a 6-well plate was transfected with 2 µg of either M.SssI methylated or unmethylated pGL2-Promoter plasmid plus pRL-SV40 control plasmid (50 ng; Promega). Where necessary, a CMV-Mecp2 expression construct (100 ng) was co-transfected. Luciferase levels were measured after ~40 h using the Dual Luciferase Assay kit according to manufacturer's instructions (Promega). Sample values were obtained according to the following formula: (luciferase sample–luciferase control)/(renilla sample–renilla control) where control values are obtained from untransfected cells. Relative luciferase values are defined as the sample value obtained using a methylated pGL-Promoter plasmid divided by the sample value obtained using the unmethylated pGL-Promoter plasmid.

Phenotypic testing and pathological analysis. Mice were analysed using the SHIRPA primary screen test series³¹ that was developed for rapid phenotype testing in mutation screens. Motor defects were tested by assaying grip strength, wire maneuver and limb tone and sensory defects by visual placing, toe pinch, corneal and pinna reflexes. Hearing was tested by the click box test. For pathological analysis, organs were examined macroscopically and solid organs were weighed. All organs sampled for histological analysis were embedded in paraffin wax, sectioned (4 µm) and stained with hematoxylin and eosin. Brain and spinal cord were additionally stained with Luxol fast blue cresyl violet stains. Tissues examined included heart, larynx, lung, liver, pancreas, tongue, esophagus, stomach, intestine, thymus, spleen, kidney, adrenal gland, testes, skeletal muscle, brain and spinal cord. The open field apparatus consisted of a rectangular box 1.5×1.0×0.2 m in size, divided into 48 (8×6) equal squares. The behavioral parameters registered during a 5 min session were as follows: (i) the total number of entries into squares (subdivided into movement in outer, middle and inner zones); (ii) the number of rears (standing on hind legs with forelegs in air or against the wall); (iii) defecation; (iv) time spent grooming; and (v) time spent immobile.

Acknowledgments

We thank D. Macleod for monitoring early mouse litters; F. Tronche and G. Schütz for *nestin-Cre* mice; J. Manson for *deleter* mice; A.J.H. Smith for ES cells; L. Vizor and J. Noble for phenotypic testing; J. Anthony and I. Davis for photographing mice; A. Greig and J. Davidson for technical assistance; staff of the Anne Walker Building for animal husbandry; A. Maas for instruction on mouse blastocyst injection; and J. Seckl, W. Skarnes, S. Brown, C. Abbott, S. Kriaucionis and J. Selfridge for advice. This work was funded by The Wellcome Trust.

Received 20 November 2000; accepted 2 February 2001.

1. Rett, V.A. Über ein eigenartiges hirnatrophisches Syndrom bei Hyperammonämie im Kindesalter. *Weiner Medizinische Wochenschrift* **37**, 723–726 (1966).
2. Hagberg, B., Aicardi, J., Dias, K. & Ramos, O. A progressive syndrome of autism, dementia, ataxia, and loss of purposeful hand use in girls: Rett's syndrome: report of 35 cases. *Ann. Neurol.* **14**, 471–479 (1983).
3. Amir, R.E. *et al.* Rett syndrome is caused by mutations in X-linked *MECP2*, encoding methyl-CpG-binding protein 2. *Nature Genet.* **23**, 185–188 (1999).
4. Amir, R.E. *et al.* Influence of mutation type and X chromosome inactivation on Rett syndrome phenotypes. *Ann. Neurol.* **47**, 670–679 (2000).
5. Wan, M. *et al.* Rett syndrome and beyond: recurrent spontaneous and familial *MECP2* mutations at CpG hotspots. *Am. J. Hum. Genet.* **65**, 1520–1529 (1999).
6. Bienvenu, T. *et al.* *MECP2* mutations account for most cases of typical forms of Rett syndrome. *Hum. Mol. Genet.* **9**, 1377–1284 (2000).
7. Cheadle, J.P. *et al.* Long-read sequence analysis of the *MECP2* gene in Rett syndrome patients: correlation of disease severity with mutation type and location. *Hum. Mol. Genet.* **9**, 1119–1129 (2000).
8. Hampson, K., Woods, C.G., Latip, F. & Webb, T. Mutations in the *MECP2* gene in a cohort of girls with Rett syndrome. *J. Med. Genet.* **37**, 610–612 (2000).
9. Huppke, P., Laccone, F., Kramer, N., Engel, W. & Hanefeld, F. Rett syndrome: analysis of *MECP2* and clinical characterization of 31 patients. *Hum. Mol. Genet.* **9**, 1369–1375 (2000).
10. Obata, K. *et al.* Mutation analysis of the methyl-CpG-binding protein 2 gene (*MECP2*) in patients with Rett syndrome. *J. Med. Genet.* **37**, 608–610 (2000).
11. Xiang, F. *et al.* Mutation screening in Rett syndrome patients. *J. Med. Genet.* **37**, 250–255 (2000).
12. Buysse, I.M. *et al.* Diagnostic testing for Rett syndrome by DHPLC and direct sequencing analysis of the *MECP2* gene: identification of several novel mutations and polymorphisms. *Am. J. Hum. Genet.* **67**, 1428–1436 (2000).
13. Lewis, J.D. *et al.* Purification, sequence and cellular localization of a novel chromosomal protein that binds to methylated DNA. *Cell* **69**, 905–914 (1992).
14. Nan, X., Tate, P., Li, E. & Bird, A.P. DNA methylation specifies chromosomal localization of MeCP2. *Mol. Cell. Biol.* **16**, 414–421 (1996).
15. Nan, X., Campoy, J. & Bird, A. MeCP2 is a transcriptional repressor with abundant binding sites in genomic chromatin. *Cell* **88**, 471–481 (1997).
16. Nan, X. *et al.* Transcriptional repression by the methyl-CpG-binding protein MeCP2 involves a histone deacetylase complex. *Nature Genet.* **37**, 386–389 (1998).
17. Jones, P.L. *et al.* Methylated DNA and MeCP2 recruit histone deacetylase to repress transcription. *Nature Genet.* **19**, 187–191 (1998).
18. Tate, P., Skarnes, W. & Bird, A. The methyl-CpG binding protein MeCP2 is essential for embryonic development in the mouse. *Nature Genet.* **12**, 205–208 (1996).
19. Meehan, R.R., Lewis, J.D., McKay, S., Kleiner, E.L. & Bird, A.P. Identification of a mammalian protein that binds specifically to DNA containing methylated CpGs. *Cell* **58**, 499–507 (1989).
20. Ng, H.-H. *et al.* MBD2 is a transcriptional repressor belonging to the MeCP1 histone deacetylase complex. *Nature Genet.* **23**, 58–61 (1999).
21. Sauer, B. & Henderson, N. Site-specific DNA recombination in mammalian cells by the Cre recombinase of bacteriophage P1. *Proc. Natl. Acad. Sci. USA* **86**, 5166–5170 (1988).
22. Schwenk, F., Baron, U. & Rajewsky, K.A. cre-transgenic mouse strain for the ubiquitous deletion of loxP-flanked gene segments including deletion in germ cells. *Nucleic Acids Res.* **23**, 5080–5081 (1995).
23. Tronche, F. *et al.* Disruption of the glucocorticoid receptor gene in the nervous system results in reduced anxiety. *Nature Genet.* **23**, 99–103 (1999).
24. Hendrich, B., Guy, J., Ramsahoye, B., Wilson, V.A. & Bird, A. Closely related proteins MBD2 and MBD3 play distinctive but interacting roles in mouse development. *Genes Dev.* (in press).
25. Fujita, N. *et al.* Methylation-mediated transcriptional silencing in euchromatin by methyl-CpG binding protein MBD1 isoforms. *Mol. Cell. Biol.* **19**, 6415–6426 (1999).
26. Ng, H.-H., Jeppesen, P. & Bird, A. Active repression of methylated genes by the chromosomal protein MBD1. *Mol. Cell. Biol.* **20**, 1394–1406 (2000).
27. Crawley, J.N. *et al.* Behavioural phenotypes of inbred mouse strains: implications and recommendations for molecular studies. *Psychopharmacology* **132**, 107–124 (1997).
28. Chen, R., Akbarian, S., Tudor, M. & Jaenisch, R. Deficiency of methyl-CpG binding protein-2 in CNS neurons results in a Rett-like phenotype in mice. *Nature Genet.* **27**, 327–331 (2001).
29. Yusufzai, T.M. & Wolffe, A.P. Functional consequences of Rett syndrome mutations on human MeCP2. *Nucleic Acids Res.* **28**, 4172–4179 (2000).
30. Free, A. *et al.* DNA recognition by the methyl-CpG binding domain of MeCP2. *J. Biol. Chem.* (in press).
31. Rogers, D.C. *et al.* Behavioral and functional analysis of mouse phenotype: SHIRPA, a proposed protocol for comprehensive phenotype assessment. *Mamm. Genome* **8**, 711–713 (1997).